

Operation of bio-aviation fuel manufacturing facility via hydroprocessed esters and fatty acids process and optimization of fuel property for turbine engine test

Gi Bo Han^{*,†}, Jung Hee Jang^{*}, Min Hwei Ahn^{*}, Young-Woong Suh^{**}, Minkee Choi^{***},
No-Kuk Park^{****}, Mi Eun Lee^{*****}, Jae-Kon Kim^{*****}, and Byunghun Jeong^{*****}

^{*}Plant Engineering Center, Institute for Advanced Engineering, Yongin-city, Gyeonggi-do 17180, Korea

^{**}Department of Chemical Engineering, Hanyang University, Seoul 04763, Korea

^{***}Department of Chemical and Biomolecular Engineering, Korea Advanced Institute of Science and Technology, Daejeon 34141, Korea

^{****}School of Chemical Engineering, Yeungnam University, Gyeongsan-city, Gyeongsangbuk-do 38541, Korea

^{*****}Alternative Fuel R&D Team, Korea Petroleum Quality & Distribution Authority, Cheongju-city, Chungcheongbuk-do 28115, Korea

^{*****}Agency for Defense Development, Daejeon 34186, Korea

(Received 5 December 2020 • Revised 15 February 2021 • Accepted 23 February 2021)

Abstract—Bio-aviation fuel to satisfy ASTM (American Society for Testing and Materials) specification was prepared through the stable operation of bio-aviation fuel manufacturing facility scale-expanded up to the production of bio-aviation fuel for turbine engine test. First, powder-typed 1.0 wt% Pt/Al₂O₃ and 0.5 wt% Pt/zeolite catalysts, respectively applicable to the hydrotreating and upgrading processes, were prepared and then their performance was evaluated in laboratory scale reactor. Thereafter, pellet-shaped 1.0 wt% Pt/Al₂O₃ and 0.5 wt% Pt/zeolite catalysts were prepared and applied to a bench-scale hydrotreating process and an upgrading process reactor, applied in the catalytic processes to prepare bio-aviation fuel. At this time, reaction characteristics under various operating conditions were investigated along with their catalytic performance evaluation. Stable long-term operation based on optimal reaction conditions, obtained in bench-scale reactor was performed using the hydrotreating process and the upgrading process reactors in a pilot-scale bio-aviation fuel manufacturing facility to continuously operate during a long time under optimal reaction conditions controlled, and then synthetic bio-crude oil including bio-aviation fuel composition was prepared. Through the separation and purification process that can selectively obtain bio-aviation fuel components, bio-aviation fuel conforming to ASTM specification standards was produced from the synthetic bio-crude oil obtained through combined hydrotreating-upgrading process.

Keywords: Bio-Aviation Fuel, Palm Oil, HEFA Process, Manufacturing Facility Operation, Fuel Properties, ASTM Standard Specification

INTRODUCTION

Carbon dioxide emissions by the global aviation industry account for about 2% of the total, and the aviation sector accounts for 12% of the total transport. Therefore, the international aviation sector is required to regulate greenhouse gas emissions and then there is a growing interest in necessary GHG reduction technologies. In 2016, the International Civil Aviation Organization (ICAO) implemented the 'CORSIA (Carbon Offsetting and Reduction Scheme for International Aviation)' to improve fuel efficiency by 2% compared to the previous year by 2050 and maintain carbon dioxide emissions at the 2020 level. It has been resolved at the 39th General Assembly and is expected to be implemented in stages from 2021. To achieve carbon-neutral growth after 2020 (CNG2020, Carbon Neutral Growth from 2020 onwards), the use of bio aviation fuel (or SAFs, Sustainable Aviation Fuels), an alternative fuel in the avia-

tion sector, which is manufactured through various processes using renewable raw materials or waste resources, takes up a large proportion [1]. Accordingly, the application of bio-aviation fuel known as carbon neutrality in the process of fuel diversification to reduce greenhouse gas in the aviation field is emerging.

To reduce recent CO₂ emissions, various research to develop technologies for manufacturing and utilizing biofuels have been continuously being conducted, and in particular, there has been much interest in developing technologies for converting low-grade bio-oils to high-grade biofuels [2-6]. The bio-aviation fuel manufacturing process includes an oil-to-jet (OTJ) that can manufacture hydrotreated esters and fatty acids (HEFA) and hydroprocessed renewable jet (HRJ) using animal and vegetable oil, alcohol-to-jet (ATJ) using alcohol, gas-to-jet (GTJ) by F-T process using syngas, and sugar-to-jet (STJ) by fermentation and catalytic conversion using sugar-based raw materials [7,8]. The HEFA process, one of the OTJ technologies, is a relatively simple process, and the bio-aviation fuel produced through it also has a high level of fuel readiness level (FRL), so it is easy to develop into a commercial technology [9-12]. Accordingly, there are many commercialized cases due to high tech-

[†]To whom correspondence should be addressed.

E-mail: gbhan@iae.re.kr

Copyright by The Korean Institute of Chemical Engineers.

nical completion, and recently it has been applied as a technology to manufacture military aviation fuel [13]. Bio-aviation fuel produced through the HEFA process exhibits similar characteristics to general petroleum products, but is known to have advantages such as high cetane number, low aromatic/sulfur content, and greenhouse gas emissions. The HEFA process is a process for converting vegetable oils such as triglycerides, which is one of the biomasses, into bio-aviation fuel through a catalytic chemical process. The detailed characteristics are as follows. First, triglycerides are known to have a structure in which three fatty acids are attached to a glycerol unit, and are currently used to convert to biodiesel (FAME, Fatty Acid Methyl Esters) through transesterification. However, since triglyceride, a molecule containing oxygen, has low thermal stability, it may cause problems when used directly as fuel for an internal combustion engine at a high concentration. In the HEFA process for bio-aviation fuel manufacturing, to overcome these shortcomings of vegetable oil, a hydrotreating process of converting to paraffin component by hydrodeoxygenation reaction that removes double bonds and oxygen components contained in vegetable oil is first required. There are three mechanisms for the hydrodeoxygenation reaction, which is the process of removing oxygen, as follows: 1) carbon monoxide and decarbonylation (DCO) converted to water, 2) decarboxylation (DCO₂) converted to carbon dioxide, and 3) hydrodeoxygenation (HDO) converted only to water. The selectivity of the three hydrodeoxygenation reaction pathways mentioned above is greatly affected by the type of metal, the type of support, and the reaction conditions, which are the active site of the catalyst. In the deoxygenation at 350 °C or higher range over a noble metal catalyst such as platinum, it is generally preferred to convert oxygen to CO or CO₂ to be removed, and thus normal-paraffin, which is one less than the length of the fatty acid, is mainly produced. Metal catalysts, which are applicable in deoxygenation, include components such as platinum (Pt), palladium (Pd), nickel (Ni), nickel-molybdenum (NiMo), and cobalt-molybdenum (CoMo) to induce hydrogenation reaction [14–27]. Another process required in the HEFA process for manufacturing bio-aviation fuel is an upgrading process that accompanies cracking and isomerization reactions to secure a hydrocarbon compound component and composition suitable for fluidity, which is one of the physical properties required for application to aviation fuel. In this process, n-paraffin, which is obtained by hydrodeoxygenation in the hydrotreating process and has a relatively high freezing point, is converted to hydrocarbons which have a liquidity corresponding to a low freezing point of below –40 °C, and a paraffin component and composition that is compatible with the existing petroleum jet fuel components. In addition, the upgrading process is accompanied by a hydrocracking reaction capable of obtaining a hydrocarbon product with a relatively short carbon length and a high isomer ratio that matches the existing petroleum jet fuel components. In the hydrocracking reaction, a bifunctional catalyst in which a metal catalyst such as Pt is supported on an acid catalyst such as zeolite is mainly used.

Research results that can produce bio-aviation fuel through HEFA process technology have been reported as follows. Verma et al. reported that bio-aviation fuel was produced from jatropha oil by applying a mesoporous Pt/SAPO-11 catalyst to the upgrading pro-

cess [28]. In addition, Liu et al. reported that a high yield of bio-aviation fuel can be obtained by using NiAg/SAPO-11 and a modified Ni/USY-MCM-41 catalyst in the upgrading process [29]. Although it succeeded in producing bio-aviation fuel by applying a Ni/zeolite catalyst, Li et al. reported that an excessive content of aromatics was detected in the bio-aviation fuel [30]. Excess aromatic components contained in bio-aviation fuels have a significant effect on the physical properties and specifications of the produced bio-aviation fuels, and even whether they are used or not, and may affect catalyst deactivation such as coking in the bio-aviation fuel manufacturing process. From the viewpoint of manufacturing bio-aviation fuel in large quantity in the long term, whether the operation stability of bio-aviation fuel manufacturing process and the physical properties and specifications of the manufactured bio-aviation fuel are satisfied can be determined by the operating state of the bio-aviation fuel manufacturing process and fuel composition and properties of produced bio-aviation fuel. Choi et al. reported that a high-yield bio-aviation fuel was successfully produced using a Pt/Nano-Beta catalyst in the upgrading process. In addition, it was reported that the bio-aviation fuel produced therefrom satisfies all required test item standards of ASTM (American Society for Testing and Materials) D7566 to be used in place of existing petroleum-based aviation fuel [31]. To use the manufactured bio-aviation fuel as a drop-in fuel with the same specifications as the existing petroleum-based aviation fuel, the evaluation and review process of a four-step process (Tier 1–4) in which the physical properties of the manufactured bio-aviation fuel comply with ASTM D4054. It must pass through and meet ASTM D7566 standards that specify the quality standards for bio-aviation fuels. Therefore, there is a need for a separation and refining process that can selectively obtain bio-aviation fuel suitable for ASTM standards corresponding to the bio-aviation fuel quality standard from the mixed bio-fuel produced from the HEFA process, which is a hydrotreating-upgrading combined process for bio-aviation fuel manufacturing.

The purpose of this study is to implement a technology for producing bio-aviation fuel that satisfies ASTM standards from palm oil, a vegetable oil. As part of this process, we tried to secure bio-aviation fuel manufacturing technology by evaluating catalyst performance at a laboratory scale, investigating reaction characteristics, and securing reaction condition corresponding to catalyst performance in a bench scale bio-aviation production process, applying to operating conditions for continuous operation in pilot scale bio-aviation fuel manufacturing facility. In addition, we attempted to confirm whether or not the ASTM standard was satisfied for the bio-aviation fuel produced by acquiring the selective fuel components contained in the mixed bio-fuel prepared from the catalytic process for producing bio-aviation fuel.

EXPERIMENTAL

1. Catalyst Preparation and Characterization

In the hydrotreating and upgrading processes for bio-aviation fuel manufacturing, 1 wt% Pt/Al₂O₃ and 0.5 wt% Pt/Z-Yt catalysts (Z-Yt: Y-type zeolite) were applied to induce hydrodeoxygenation and hydrocracking reactions, respectively. These catalysts were prepared by the impregnation method as follows. The precursor and

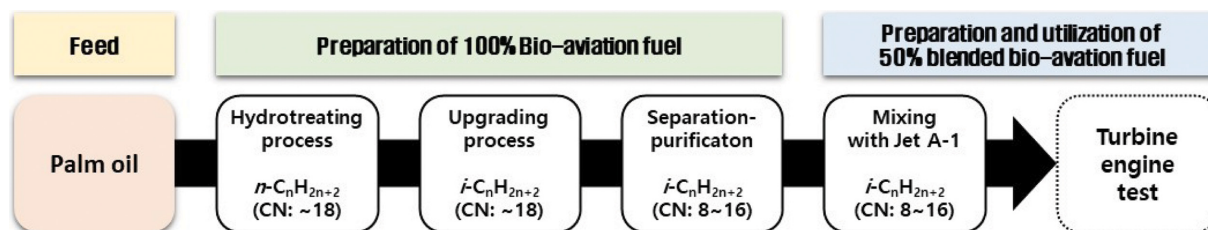


Fig. 1. Schematic diagram of bio-aviation fuel manufacturing process including hydrotreating, upgrading, separation-purification and fuel property optimization (CN: carbon number).

support of 1 wt% Pt/Al₂O₃ were tetraammineplatinum(II) nitrate (H₁₂N₆O₆Pt, Alfa acer) and Al₂O₃ (Strem Co. Ltd., length: 3 mm, diameter: 3 mm, pellet type), respectively. Also, the precursor and the support of 0.5 wt% Pt/Z-Yt catalyst for upgrading process were tetraammineplatinum(II) nitrate (H₁₂N₆O₆Pt, Alfa acer) and Y-type zeolite (Z-Yt, length: 3-5 mm, diameter: 1.2 mm, cylinder type), respectively. Pt precursors in an amount corresponding to 1 wt% and 0.5 wt% Pt relative to the weight of Al₂O₃ and Z-Yt supports for the hydrotreating and upgrading, respectively, were mixed with an appropriate amount of distilled water to prepare an aqueous solution under stirring for a sufficient time. After that, the Al₂O₃ support for the catalyst for the hydrotreating process and the Z-Yt support for the upgrading process were, respectively, added to allow the Pt precursor component in the aqueous solution to be absorbed into the support. After an appropriate period of time, the Al₂O₃ and Z-Yt impregnated with the Pt precursor were separated from the aqueous solution, followed by drying at 110 °C overnight and sintering at 400 °C for 4 h, and then 1 wt% Pt/Al₂O₃ (1PA) catalyst for hydrotreating process and 0.5 wt% Pt/Z-Yt (0.5PZ) catalyst for upgrading process were prepared, respectively. The 1PA and 0.5PZ catalysts obtained after calcination were selectively classified to have a particle size of 1 to 1.5 mm through a crushing process, and then filled into bench and pilot scale reactors for hydrotreating and upgrading processes, respectively, and used.

X-ray diffraction (XRD) analysis was performed using the radiation of Cu K α , 40 kV and 15 mA of Rigaku miniFlex600 equipment, and the scan speed and step size were 10°/min and 0.02°, respectively. Brunauer-Emmett-Teller (BET) analysis was performed using a Micromeritics ASAP 2020 instrument to measure the surface area, pore volume, and pore size of the support and catalyst through N₂ physisorption. The sample was pretreated at 105 °C for 1 h in a vacuum state. The specific surface area was calculated by the BET equation under the pressure condition of P/P₀ being 0.05-0.2, and the micropore volume was calculated by t-plot. The total pore volume was measured at P/P₀=0.98, and the mesopore volume was calculated by excluding the micropore volume from the total pore volume.

After pyridine adsorption, infrared spectroscopy was performed to qualitatively and quantitatively analyze the type and amount of acid sites of the catalyst. A Nicolet iS50 (Thermo Fisher) instrument equipped with an in-situ cell was used, and before analysis, about 20 mg of a sample was fixed in the cell in the form of a thin pellet and pretreated under vacuum at 400 °C for 4 h. After that, the pyridine vapor was adsorbed at 150 °C for 1 h, and then the adsorption was terminated and placed under vacuum at the same

temperature for 2 h to desorb the weakly adsorbed pyridine and proceed with the analysis. As a result of the measured infrared spectroscopy, it was divided into Brönsted and Lewis acid sites and analyzed qualitatively and quantitatively (Brönsted acid site: 1,545 cm⁻¹ (ϵ =1.67 cm/ μ mol), Lewis acid site: 1,455 cm⁻¹ (ϵ =2.22 cm/ μ mol)). CO chemisorption analysis was performed using BELCAT-B equipment to measure the dispersion and particle size of Pt. After pretreatment for 1 h in a 10% H₂/Ar (30 cm³/min) atmosphere at 150 °C, lower the temperature to 30 °C in a He (30 cm³/min) atmosphere. After that, 5% CO/He is injected in a pulse and adsorbed until saturated.

2. Hydrotreating and Upgrading Processes Operation with Various Scale

The bio-aviation fuel manufacturing process in this study consists of elemental processes such as a hydrotreating process to induce a hydrodeoxygenation that can generate n-paraffin from vegetable oil, upgrading process to induce hydrocracking that can produce a mixed bio-crude oil, including bio-aviation fuel from n-paraffin, and separation and refining process that can selectively obtain bio-aviation fuel from a mixed bio-crude oil. And, these elemental processes were separately fabricated and were operated, individually and in conjunction for bio-aviation fuel. Fig. 1 shows the schematic diagram of bio-aviation fuel manufacturing process including hydrotreating, upgrading, separation-purification and fuel property optimization applied in this study.

Each reaction system used for the hydrotreating and upgrading process includes a feed container with an externally mounted heater capable of fluidizing and a raw material supply line equipped with a high-pressure pump capable of injecting raw materials for smooth supply of raw materials. In addition, it includes a high-pressure gas cylinder capable of supplying H₂ for hydrogenation reaction, H₂ supply line equipped with a mass flow controller (MFC), and pre-heater to sufficiently reach the reaction temperature by confluence of these raw materials and H₂. The reactor is a fixed bed TBR type that is installed vertically so that the raw material can flow from top to bottom through the catalyst bed by filling the amount of catalyst corresponding to the space velocity (WHSV) relative to the amount of raw material to be supplied. In addition, a thermocouple was installed inside the reactor to measure the internal temperature, and a furnace was installed outside the reactor to supply a heat source to the catalyst layer inside the reactor. At the rear end of the reactor, a back pressure regulator (BPR) was installed to control the pressure inside the reactor, and a liquid recovery vessel capable of gas-liquid separation was installed. In addition, temperature and pressure sensors were located in each necessary part

Table 1. Operating conditions for laboratory, bench, and pilot scale reaction system for hydrotreating and upgrading processes

Process		Hydrotreating			Upgrading		
Feed		Palm oil			n-Paraffin (C15-C18)		
Product		n-Paraffins (C15-C18)			(i+n)-Paraffins (C5-C17)		
Catalyst		1PA			0.5PZ		
Scale		Lab.	Bench	Pilot	Lab.	Bench	Pilot
Amount of catalyst packed (g)		1	90	900	1.25	60	600
Catalyst type		Powder	Pellet	Pellet	Powder	Pellet	Pellet
Temperature (°C)		380	375-395	385-400	243	233-247	240-245
Operation condition	Pressure (bar)	40	40	40	50	50	40
	Space velocity (h ⁻¹ , WHSV)	2.0	2.0	2.0	2.0	2.0	2.0
	H ₂ /Feed ratio (mol/mol)	50.0	32.0	32.0	16.7	16.8	16.8

to monitor temperature and pressure in real time, and a temperature-pressure monitoring-control system that can collect corresponding data in real time was installed. Fixed-bed catalytic reactors for hydrotreating and upgrading processes are used differently in laboratory, bench, and pilot scales according to the manufacturing scale of bio-aviation fuel, and the amount of catalyst backed in the hydrotreating/upgrading reactor was 1/1.25, 90/60 and 900/600 g, respectively. Table 1 lists the range of operating conditions for laboratory, bench, and pilot scale facilities for the reaction system for hydrotreating and upgrading processes for manufacturing bio-aviation fuel.

3. Product Analysis in Hydrotreating and Upgrading Processes

The product produced in the hydrotreating and upgrading process was recovered from the liquid recovery container, and the total liquid product yield (wt%) was calculated through weight measurement. In addition, the hydrocarbon yield (wt%) was calculated by separating the hydrocarbon in the liquid product. A sample for analysis was prepared by mixing 0.2 mL of the product, 0.2 mL of a standard sample, 0.2 mL of dodecane, and 1 mL of chloroform as a solvent to prevent solidification of the product. GC analysis was performed using a YL6500 instrument equipped with an HP-5 column and an FID detector. The temperature of the inlet and the detector was 320 °C, and the oven was analyzed under the conditions of raising the temperature at 10 °C/min from 80 °C to 310 °C and holding for 15 minutes. In addition, a qualitative analysis of the unknown material was performed through a GC-MS (Agilent 7890A, MS 5975C) instrument. Analysis was performed in EI mode on the HP-5MS column, and the analysis conditions were inlet 280 °C and the oven temperature was increased from 40 to 250 °C at 2 °C/min.

4. Distillation Process for Separation of Bio-Aviation Fuel

A separation-purification process is required to separate bio-aviation fuel with optimized physical properties required by ASTM standards from bio-crude oil produced from palm oil through the sequential operation of hydrotreating and upgrading processes. In this study, the distillation process was applied as a separation and purification process to secure the composition of bio-aviation fuel from bio-crude oil. The feed tank and condenser capacity included in the distillation facility were 20 and 2 L, respectively, and the

diameter and length of the distillation column were 50 mm and 1,200 m, respectively. The reflux ratio is adjustable from 1 to 10, and the maximum operating temperature is 400 °C. To secure the composition of bio-aviation fuel from bio-crude oil, the initial temperature controlled under the condition of normal pressure was about 205 to 210 °C, and the end temperature was in the range of 275 to 280 °C.

RESULTS AND DISCUSSION

1. Palm Oil Characterization

The major physical properties of palm oil, a raw material for bio-aviation fuel, were analyzed, and the glyceride (mono, di, tri)-based alkyl-based structure of palm oil was examined through gas chromatography analysis. Fig. 2 shows GC chromatography results of analyzing the fatty acid structure. As a result, the fatty acid structure in the raw material was more than 45% of C16:0 and C18:0 content such as saturated fatty acids (SFA, Saturated Fatty Acids), but they contain double bonds, so oxidation stability is weak, as well as deoxygenation. The content of the unsaturated fatty acids C18:1 and C18:2, which can cause an increase in the amount of H₂ injected, was also measured to be 38% and 10%, respectively, due to the additional reaction accompanying saturation of the bond structure during the reaction. Also, main physical properties of palm oil used as a raw material for producing the bio-aviation fuel are shown in Table 2. The properties of palm oil were as follows: 1) Total acid number: 0.22 mg/mg_{KOH}, 2) iodine value: 55.5 g/100 g, 3) Na/K content: N.D, 4) Ca content: 0.63 mg/kg, 5) gross calorific value: 8,612 kcal/kg, 6) carbon content: 77 wt%, 7) hydrogen content: 12 wt%, 8) oxygen content: 10 wt%.

2. Characterization of 1PA and 0.5PZ Catalysts

Fig. 3 shows the physico-chemical properties of 1PA catalyst and γ -Al₂O₃ support. As shown in Fig. 3(a), XRD analysis results of γ -Al₂O₃ used as a support and the 1PA catalyst applied to the hydrotreating process, the alumina support without Pt component was found to be gamma alumina. Also, the crystallinity of the Pt component was not confirmed, and only the peak of γ -Al₂O₃ appeared even in the case of the 1PA catalyst in which 1 wt% Pt was supported on the gamma alumina support. This is believed to

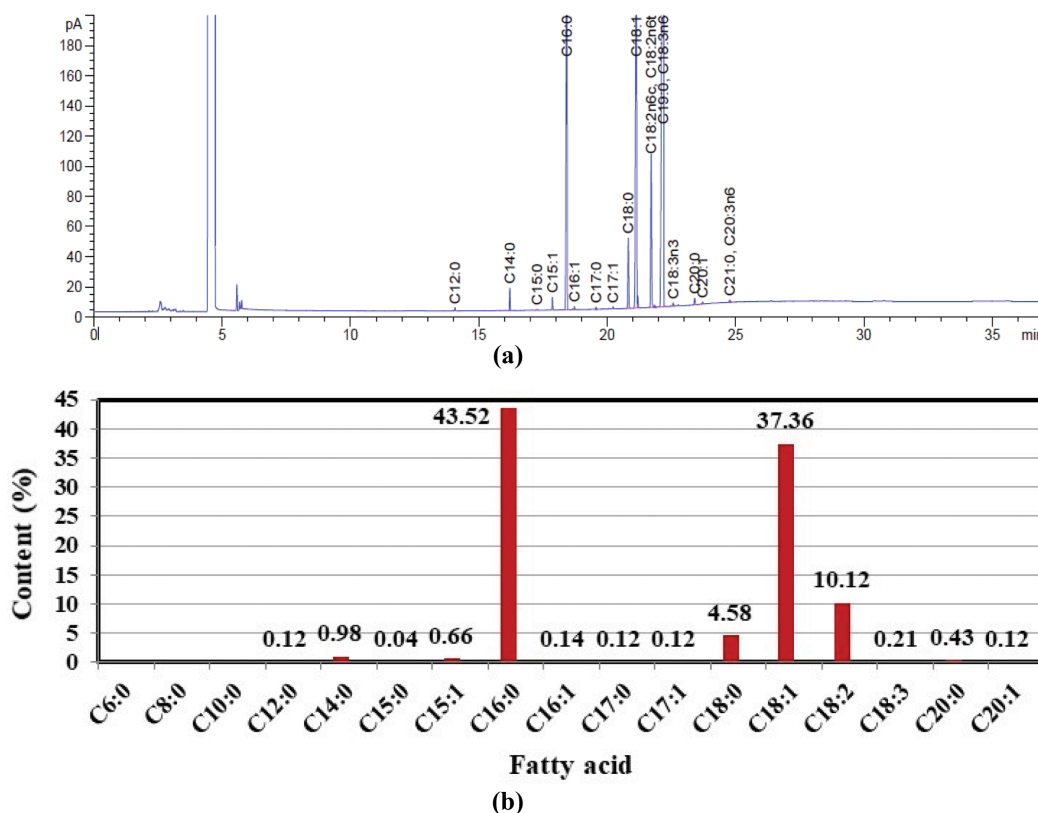


Fig. 2. GC chromatography results of analyzing the fatty acid structure of palm oil used as a raw material for production of bio-aviation fuel ((a) GC chromatograph, (b) content of fatty acids).

Table 2. Physical properties of palm oil

Property	Unit	Result	
Flash point	°C	262	
kinematic viscosity (50 °C)	mm ² /s	41.35	
Carbon residue content	wt%	0.78	
Ash content	wt%	0.02	
Sulfur content	wt%	0.01	
Nitrogen content	wt%	0.0001	
Pour point	°C	12	
Density (@15 °C)	kg/m ³	915.5	
Moisture and impurities	wt%	0.01	
Total acid number	mg _{KOH} /g	0.22	
Iodine value	g/100 g	55.5	
Alkali metal content	Na	mg/kg	Not detected
	Ca	mg/kg	0.63
	K	mg/kg	Not detected
Gross calorific value	kcal/kg	8,612	
Carbon content	wt%	77	
Hydrogen content	wt%	12	
Oxygen content	wt%	10	

be because the Pt component was not only supported in a low content of 1 wt%, but also dispersed with a relatively high degree of dispersion, so that crystallinity could not be detected. As shown

in Fig. 3(b) of the TEM image of the IPA catalyst to observe the size of the Pt particles supported on the alumina support, it can be seen that the average size of Pt particles formed on the alumina support is about 1.6 nm. Fig. 3(c) shows the results of infrared spectroscopy after pyridine adsorption to qualify and quantify the types and amounts of acid sites of alumina support and IPA catalyst. It was confirmed that the amount of the acid site of the IPA catalyst decreased with the metal Pt support compared to only γ -Al₂O₃ support, and there was an abundant number of Lewis acid sites, whereas there was almost no Brønsted acid site. The Lewis acid sites of the γ -Al₂O₃ support and the IPA catalyst was 130.3 and 107.1 μ mol/g, respectively. The detailed pyridine adsorption analysis results can be seen in Fig. 3(c) showing the pyridine adsorption curve. From the morphological analysis results of the Al₂O₃ support and the IPA catalyst, it was confirmed that there was no significant difference in surface area and pore volume regardless of whether or not Pt was supported because the supported Pt content of the IPA catalyst was very low.

Fig. 4 shows the physico-chemical properties of Z-Yt as a support of 0.5PZ catalyst applied to the upgrading process. γ -Al₂O₃ support. As shown in Fig. 4(a) of the XRD pattern of the zeolite-based Z-Yt support used as the catalyst support in the upgrading process, it was confirmed that the zeolite-based Z-Yt support had the specific peak of the Y-type zeolite having an FAU structure and almost no impurities were observed. As shown in Fig. 4(b) of the TEM image to observe the pore characteristics of the zeolite-based Z-Yt support, it was confirmed that the zeolite-based Z-Yt sup-

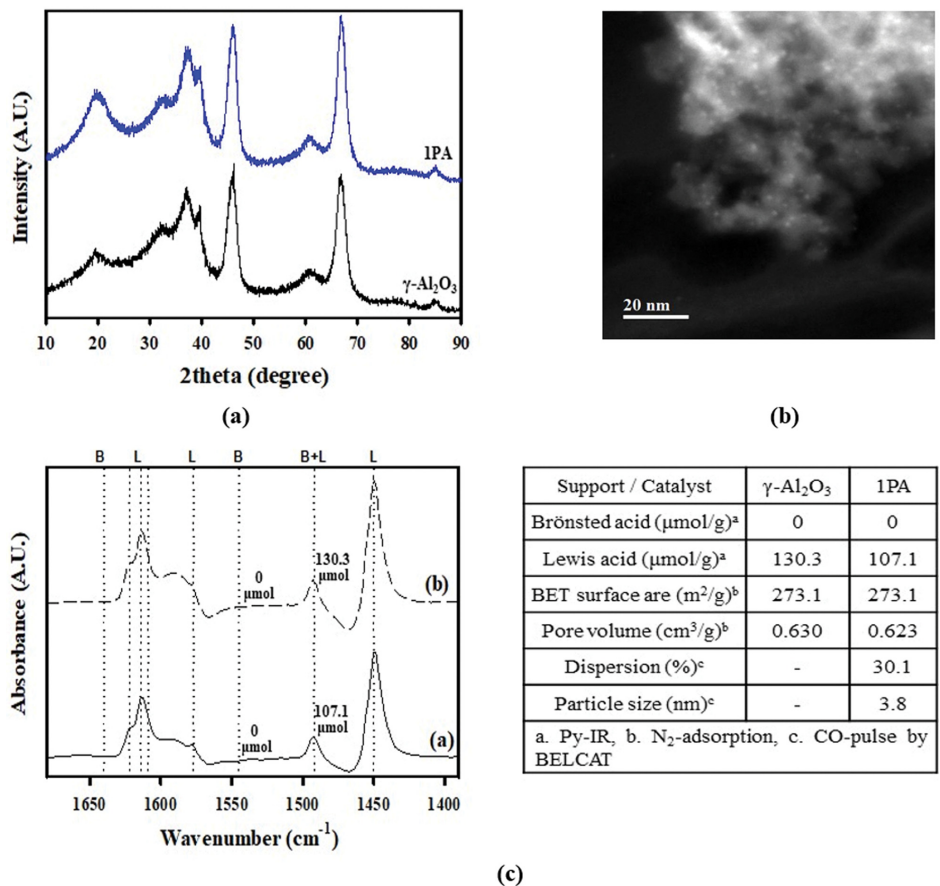


Fig. 3. Physico-chemical properties of IPA catalyst and γ -Al₂O₃ support ((a) XRD patterns, (b) TEM image, (c) acid site properties).

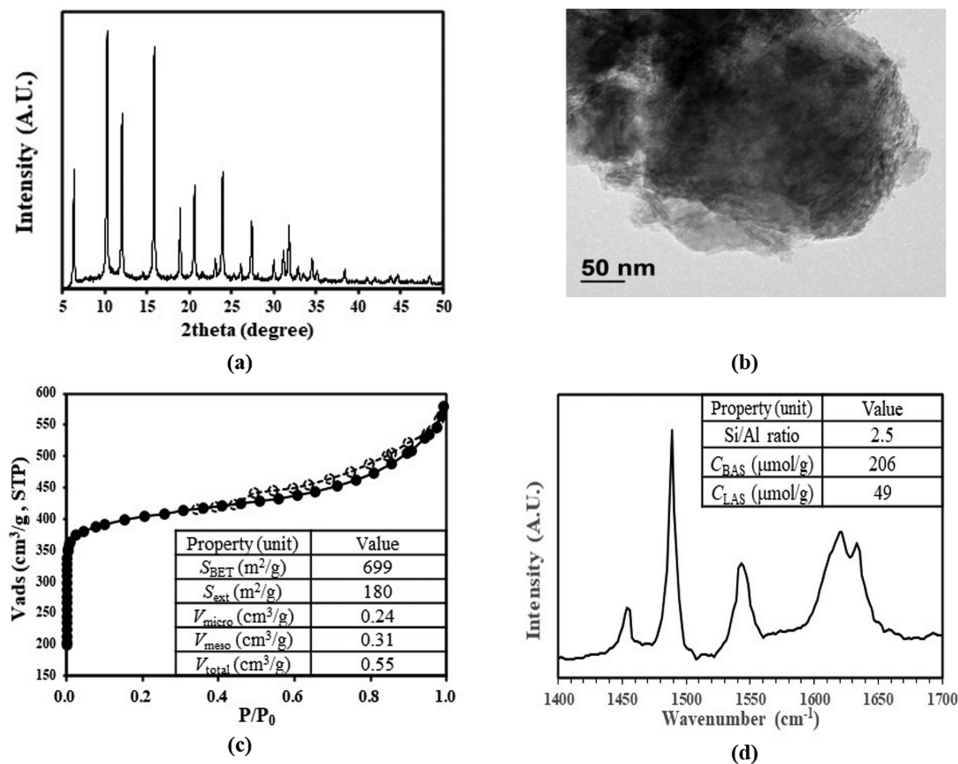


Fig. 4. Physico-chemical properties of Z-Yt support ((a) XRD pattern, (b) TEM image, (c) morphological properties, (d) acid site properties).

port had well developed mesopores. In addition, the surface was covered with an alumina binder in consideration of the molded support. As shown in Fig. 4(c) of the N_2 -physical adsorption isotherm curve to characterize the pore structure of the zeolite-based Z-Yt support, it was known that the Si/Al ratio of the pellet-type Z-Yt zeolite support was about 2.5-2.8, and the surface area and micropores of the catalyst were reduced, and the mesopores volume did not appear to be largely changed. This means that the alumina component used as the binder partially blocked the micropores of the Z-Yt support. As shown in Fig. 4(d) of the type and amount of acid sites of zeolite-based Z-Yt support using infrared spectroscopy after pyridine adsorption, it was estimated that the distribution and amount of the Brönsted and Lewis acid sites are due to the Si/Al ratio of the zeolite support. Considering that the Si/Al ratio of the Z-Yt support was 2.5, the amount of the Brönsted acid site was $206 \mu\text{mol/g}$ and the amount of the Lewis acid site was $49 \mu\text{mol/g}$.

Table 3 shows the Pt properties and the ratio of activated Pt to the Brönsted acid site of the 0.5PZ catalyst used for the hydrocracking reaction in the upgrading process. The supported Pt prop-

Table 3. Pt properties and the ratio of activated Pt to the Brönsted acid site of the 0.5PZ catalyst

Property	Pt (wt%)	H/Pt	nPt/nC _{BAS} (mol/mol)
Value	0.5	1.03	0.13

erties of the 0.5PZ catalyst prepared by supporting 0.5 wt% Pt on a zeolite-based Z-Yt support were analyzed through H_2 chemisorption. As can be seen from the table, the H/Pt value is 1.03, which means that the supported Pt is uniformly and evenly dispersed on the surface of the support with a small size of about 1 nm. On the other hand, the ideal catalyst for hydrocracking has a catalytic property that a metal site for hydrogenation/dehydrogenation is stronger than an acid site for decomposition of a C-C bond. For the 0.5PZ catalyst, the molar ratio of Pt to the Brönsted acid site (nPt/nCBAS) was calculated to investigate the catalytic properties of the metal site and the acid site. The nPt/nCBAS value of the 0.5PZ catalyst was 0.13, which is much more than the nPt/nCBAS value of 0.05 proposed by Guisnet et al. [32]. Through this analysis result, it can be said that the 0.5PZ catalyst used for the upgrad-

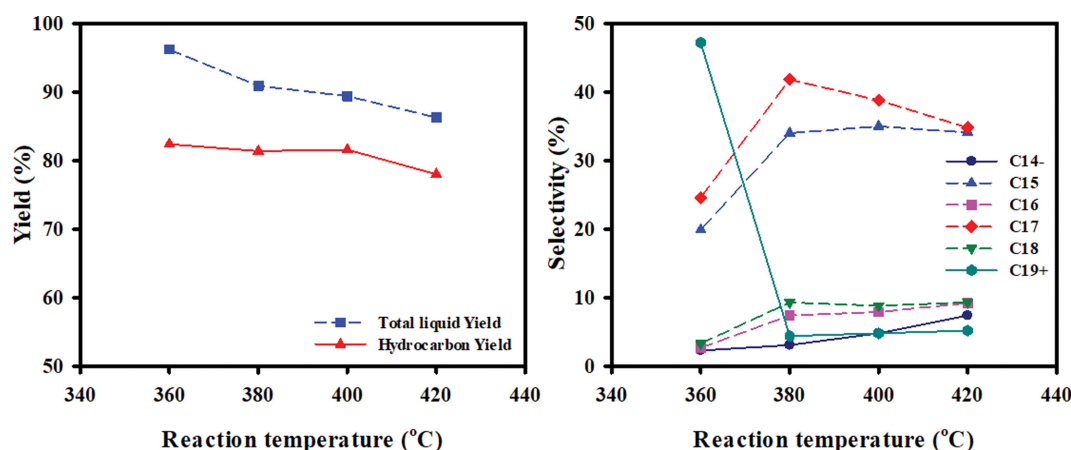


Fig. 5. Effect of reaction temperature on reaction characteristics in a laboratory-scale hydrotreating process using IPA catalyst (Reaction pressure: 40 bar, space velocity (WHSV): 2.0 h^{-1} and H_2 /reactant ratio: 50).

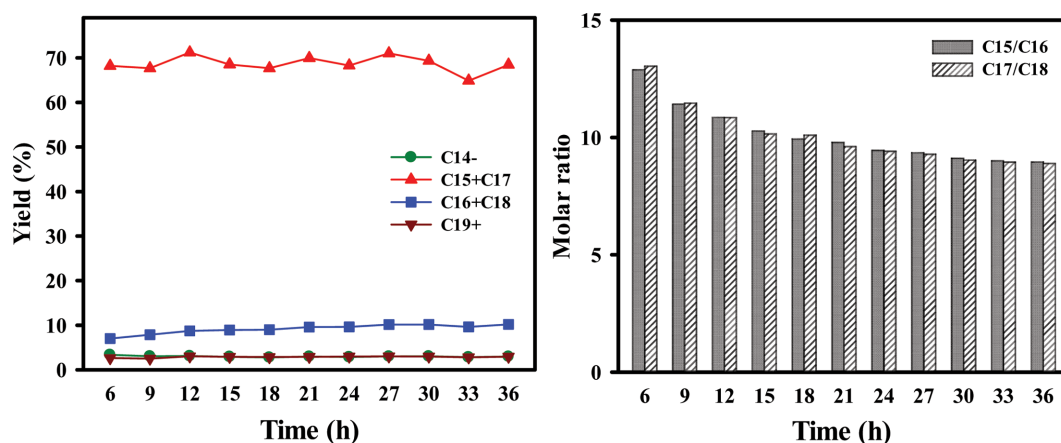


Fig. 6. Long-term performance stability of IPA catalyst in a laboratory scale hydrotreating process (Reaction temperature: 380°C , reaction pressure: 40 bar, space velocity (WHSV): 2.0 h^{-1} and H_2 /reactant ratio: 50).

ing process in this study is suitable for the hydrocracking reaction.

3. Catalyst Performance Test in Laboratory-scale Reactor

Fig. 5 shows the effect of reaction temperature on reaction characteristics while 1PA was used in a laboratory-scale hydrotreating process. With changing the reaction temperature to 360–420 °C under the conditions of reaction pressure, space velocity and H_2 /reactant ratio of 40 bar, $2.0 h^{-1}$, and 50, respectively, the yield of hydrocarbon and the composition of the hydrocarbon were observed with the change in reaction temperature. At 360 °C, palm oil conversion was not 100%, and then fatty acids (Palmitic acid, Stearic acid), the intermediates, remaining in the product, resulted in

C19+ selectivity reaching 47.2%. On the other hand, at a relatively high reaction temperature of 420 °C, a relatively low hydrocarbon yield of 78.0% was obtained. Above 380 °C excluding 360 °C, the C17 selectivity decreased from 40.3 to 34.8% and the selectivity of C14–, which are hydrocarbons having 14 or less carbon number, increased from 3.6 up to 7.4% as the reaction temperature increased from 380 to 420 °C. It was estimated that this is due to the reaction characteristic of decomposing a relatively high carbon number hydrocarbon compound produced by conversion of palm oil as the reaction temperature increases. In addition, in particular, in the reaction temperature range of above 400 °C, the increas-

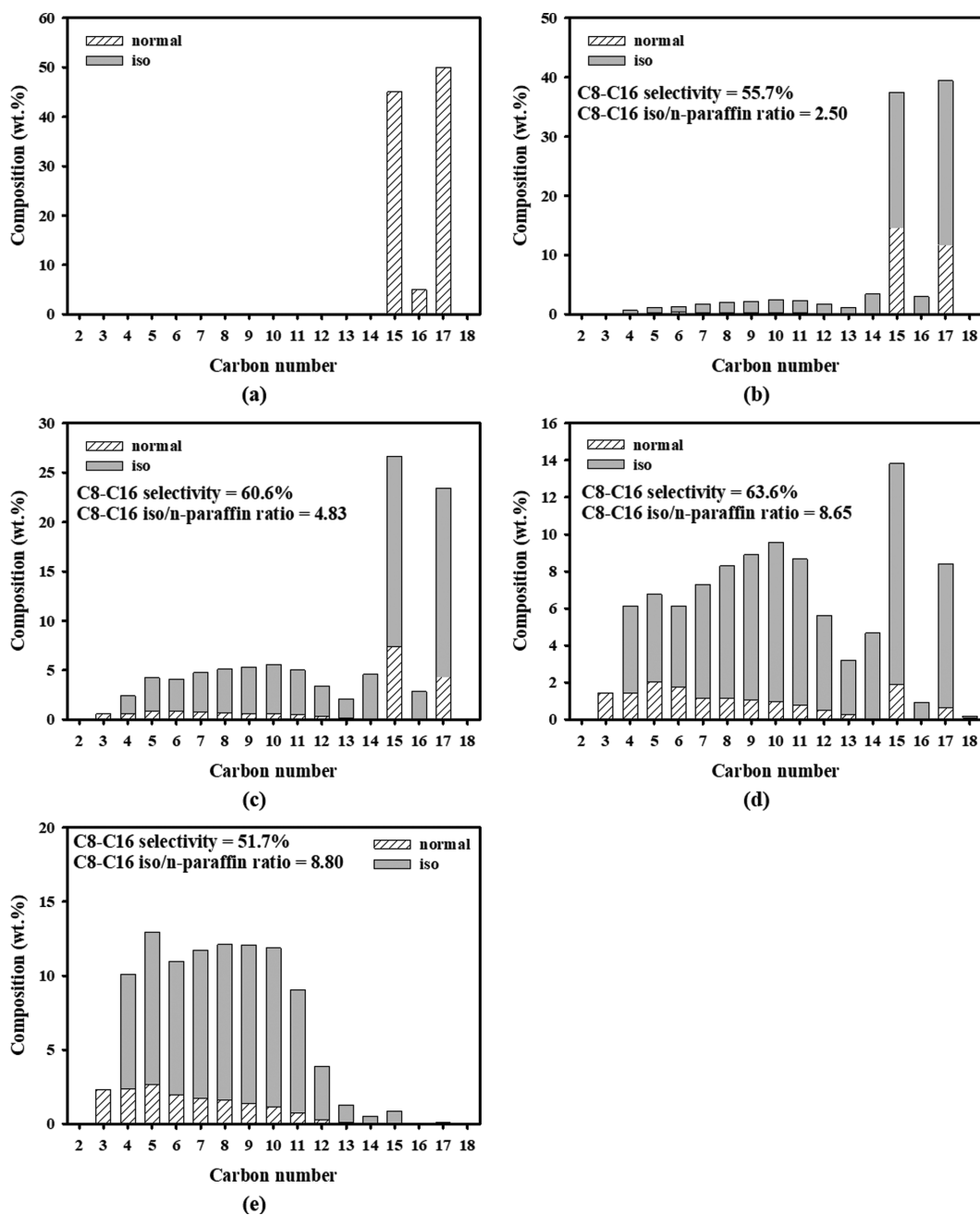


Fig. 7. Effect of reaction temperature on reaction characteristics in the upgrading process using 0.5PZ catalyst ((a) Reactant, (b) 240 °C, (c) 245 °C, (d) 250 °C, (e) 255 °C, reaction pressure: 50 bar, space velocity (WHSV): $2.0 h^{-1}$, H_2 /reactant ratio: 16.8).

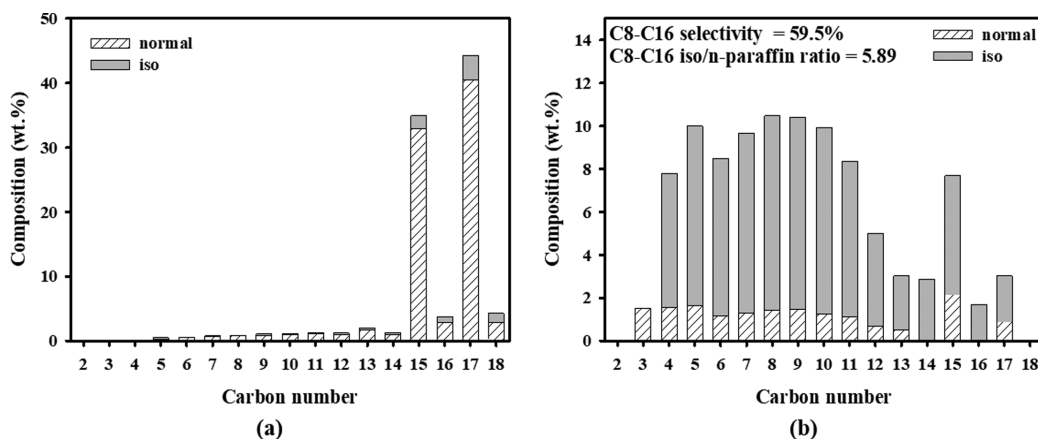


Fig. 8. Hydrocracking reaction characteristics over 0.5PZ catalyst in the upgrading process using the hydrocarbons, as an actual feed, produced from palm oil by the hydrotreating process ((a) Reactant, (b) 250 °C, reaction pressure: 50 bar, space velocity (WHSV): 2.0 h⁻¹, H₂/reactant ratio: 16.8).

ing rate of C14~ selectivity as the reaction temperature rises was high, so that the hydrocarbon yield and C17 selectivity were relatively low. Therefore, it was estimated that the appropriate reaction temperature range to obtain hydrocarbons with a relatively high carbon number that can be used as a reactant in the subsequent upgrading process in high yield is from 380 to 400 °C in the laboratory-scale hydrotreating process using the 1PA catalyst.

Fig. 6 shows the long-term performance stability of 1PA catalyst in a laboratory scale hydrotreating process. Reaction conditions were reaction temperature, reaction pressure, space velocity (WHSV) and H₂/reactant ratio of 380 °C, 40 bar, 2.0 h⁻¹ and 50, respectively. In the hydrotreating process using 1PA catalyst at 380 °C, the yield of n-paraffins of C15-C18 corresponding to the catalytic deoxygenation reaction characteristics was about 75.2-78.7%. Among them, the yield of C15+C17 n-paraffins generated through the reaction pathway of DCO and DCO₂ was about 68%. In addition, the n-paraffin yield of C16+C18 generated by the reaction path of HDO was 7.0% at the beginning of the reaction and increased to 10.2% at the end. The molar ratio of C15/C16 and C17/C18 decreased from 13.0 to 9.0 with the passage of the reaction time. The yield of the ~C14 n-paraffin with relatively low carbon number and the C19~ n-paraffin with relatively high carbon number was about 3.1 and 2.8%, respectively, and they remained stable during the reaction time. From these reaction characteristics results, it was confirmed that the 1PA catalyst performance was maintained at 380 °C in the hydrotreating process, and then the reaction temperature of 380 °C was appropriate and the 1PA catalyst performance was stable for a long time.

The effect of reaction temperature on a laboratory-scale upgrading process using a 0.5PZ catalyst capable of producing a fuel component of bio-aviation fuel from a model reactant simulating a hydrocarbon compound generated from palm oil by a hydrotreating process was investigated. Fig. 7 shows the effect of reaction temperature on reaction characteristics in the upgrading process using 0.5PZ catalyst. In the upgrading process accompanied by hydrocracking and hydroisomerization reactions under the application of 0.5PZ catalyst, the effects on the carbon number distribution, iso/n ratio, and C8-C16 yield by varying the reaction tem-

perature were investigated. As the reaction temperature increased, the selectivity of n-C15-C17 paraffin gradually decreased, and the selectivity of the iso-C15-C17 and ~C15 products gradually increased. This tendency means that the reactivity of the hydroisomerization and hydrocracking simultaneously increases as the reaction temperature increases. In addition, in the region of a relatively low reaction temperature, the reaction temperature rises and the hydroisomerization reaction is more dominant, and in the region of the relatively high reaction temperature, the reaction temperature rises and the hydrocracking reaction tends to dominate. At a reaction temperature of about 255 °C, the n-C17 paraffin component was not observed, and it was estimated that the conversion reached about 100%. At the reaction temperature of 250 °C, the content of n-C17 was about 8.7%, and the conversion did not reach about 100%; however, a high C8-C16 yield of 63.6 wt% and a high iso/n-paraffin ratio of 8.65 were obtained. From these results, it was determined that the appropriate reaction temperature for the upgrading process using the 0.5PZ catalyst was around 250 °C.

Fig. 8 shows the hydrocracking reaction characteristics over 0.5PZ catalyst in the upgrading process using the hydrocarbons, as an actual feed, produced from palm oil by the hydrotreating process. As shown in Fig. 8, unlike the model reactants previously applied as raw materials, the content of C5-C14 corresponding to with a relatively low carbon number distribution in the hydrocarbons produced from palm oil through the hydrodeoxygenation in the hydrotreating process was about 10 wt% and iso-paraffin was partially mixed with n-paraffin. The reaction temperature of 250 °C was selected based on the effect of reaction temperature on the hydrocracking of the upgrading process obtained in Fig. 8. In the laboratory-scale upgrading process using 0.5PZ catalyst carried out at 250 °C, a mixed bio-crude oil including bio-aviation fuel component corresponding to the C8-C16 yield of 59.5% and the iso/n-paraffin ratio of 5.89 was obtained from the actual feed.

In general, catalytic performance with long-term stability is required for stable bio-aviation fuel production. In addition, it is known to help maintain catalytic activity by applying a catalyst having a high metal/acid ratio and a reaction condition having a high H₂/reactant ratio in the hydrocracking reaction of n-paraffin.

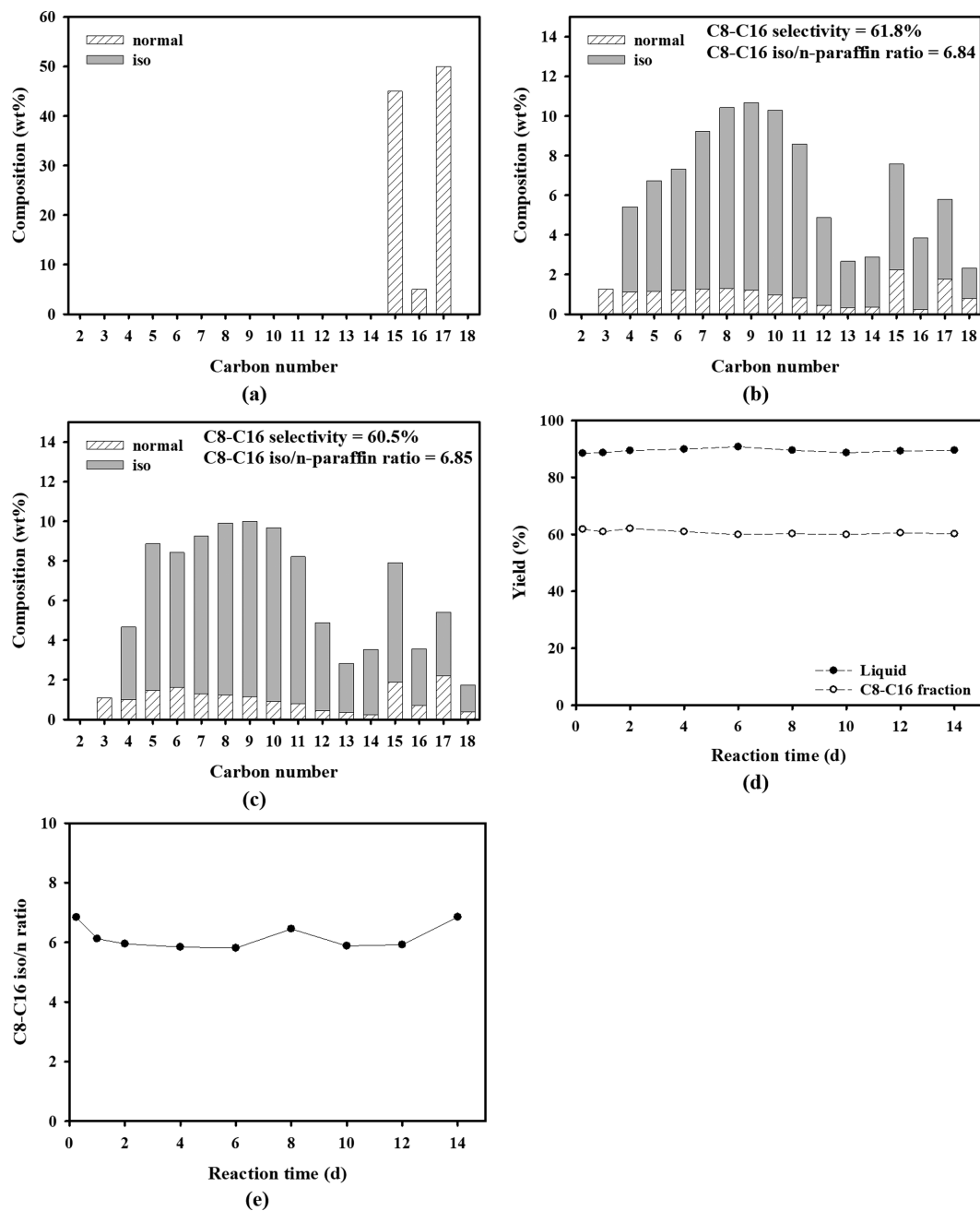


Fig. 9. Long-term stability of catalyst performance in upgrading process using 0.5PZ catalyst for 2 weeks ((a) Reactant, (b) 0.25 d, (c) 14 d, (d) yield, (e) iso/n-paraffin ratio, reaction temperature: 250 °C, reaction pressure: 50 bar, space velocity (WHSV): 2.0 h⁻¹, H₂/reactant ratio: 16.8).

The actual feed, which is manufactured from palm oil by the hydrotreating process and used as a reactant in the upgrading process, contains non-paraffinic components other than normal-paraffin in an amount of about 5 wt%. These non-paraffinic components may include olefins, aromatics, and fatty acids that have not been converted by a hydrodeoxygenation reaction in a hydro-treating process. When a feed containing a non-paraffinic component is used as a reactant in the upgrading process, it may affect the long-term stability of the catalyst, and thus act as an important factor in manufacturing bio-aviation fuel. Fig. 9 shows the results of observing the long-term stability of catalyst performance

while operating the laboratory-scale upgrading process using 0.5PZ catalyst for 2 weeks. As reaction conditions, reaction temperature, reaction pressure, space velocity, and H₂/reactant ratio were 250 °C, 50 bar, 2.0 h⁻¹, and 16.8, respectively. As shown in Fig. 9(b)-(c), there is little difference in the composition of paraffin in the product obtained at the beginning (0.25 days) and at the end (14 days) after the start of the reaction. Non-paraffinic components of C19+ included in the feed obtained after the hydrotreating process and applied as an actual reactant in the upgrading process were not observed in the product after the upgrading process. This fact means that non-paraffinic components were converted into paraf-

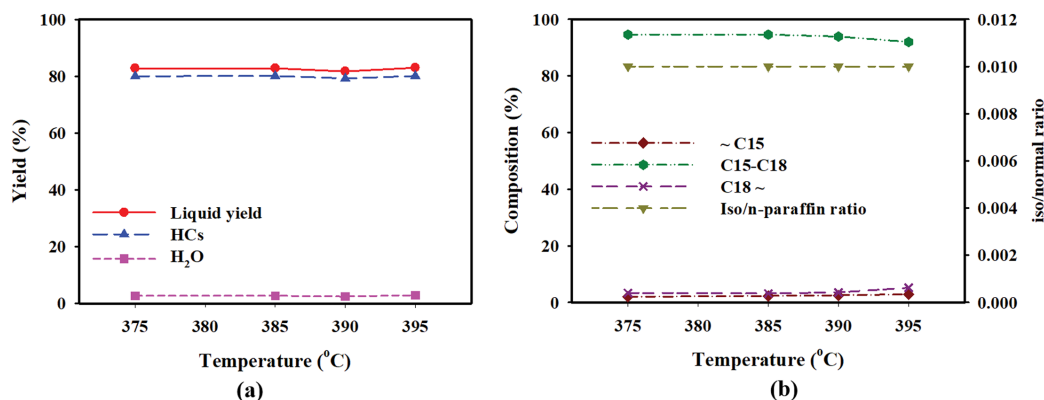


Fig. 10. Effect of reaction temperature on the reaction characteristics for a bench-scale hydrotreating process using 1PA catalyst ((a) Yield of liquid product, hydrocarbons and H₂O, (b) selectivity of hydrocarbon with carbon number and iso/n-paraffin ratio, reaction pressure: 40 bar, H₂/reactant ratio: 32, space velocity (WHSV): 2.0 h⁻¹).

finic components by deoxygenation and hydrogenation that were additionally performed simultaneously with the hydrocracking in the upgrading process. In addition, as the reaction time elapsed, the yield of the liquid product and the composition of the bio-aviation fuel containing it, and the iso/n-paraffin ratio of the composition of the bio-aviation fuel were observed. Throughout the reaction time for monitoring catalytic performance, both the yield of the liquid product and the bio-aviation fuel composition were kept constant, and the iso/n-paraffin ratio in the product was also maintained at an almost constant value of 6.3 ± 0.5 . Through these results, it was determined that the long-term stability of 0.5PZ catalyst performance for the upgrading process was secured.

4. Operation of Bench-scale Hydrotreating and Upgrading Processes

Fig. 10 shows the effect of reaction temperature on the reaction characteristics for a bench-scale hydrotreating process using 1PA catalyst. While the reaction pressure, H₂/reactant ratio, and space velocity were fixed, the liquid product yield and hydrocarbon composition were monitored along with the reaction temperature change. The reaction pressure, H₂/reactant ratio and space velocity were fixed at 40 bar, 32, 2.0 h⁻¹, etc., and the reaction temperature was changed from 375 to 395 °C based on the temperature of the catalyst bed inside the reactor. The palm oil conversion reached 100% regardless of the reaction temperature change within the reaction temperature range for the investigation of the reaction characteristics, and the result is not shown in the graph. The liquid product recovered as a hydrotreating product, and n-paraffin of C15-C18, which are hydrocarbons that will be used as actual reactants in the upgrading process, and moisture were quantified and their yield and the composition of n-paraffins of C15-C18 were confirmed. Although the reaction temperature was changed to 375, 385, and 395 °C, the liquid product yield was almost unchanged at about

83, 81, and 82%. On the other hand, in the paraffin composition contained in the liquid product along with the reaction temperature change, the paraffin selectivity of less than 15 carbon number was not significantly affected by the reaction temperature; however, the paraffin selectivity of C15 to C18 slightly decreased with the increase of the reaction temperature. The selectivity of a hydrocarbon compound product having a carbon number of more than 18 also slightly increased as the reaction temperature increased. The iso/n-paraffin ratio hardly changed in spite of the temperature change, and it is believed that side reactions other than hydrodeoxygenation hardly occurred in the bench-scale hydrotreating process using 1PA catalyst.

Fig. 11 shows the effect of reaction temperature on the reaction characteristics in a bench-scale upgrading process using 0.5PZ catalyst. While the reaction pressure, H₂/reactant ratio, and space velocity were fixed, the liquid product yield and paraffin composition were investigated along with the reaction temperature change. The reaction pressure, H₂/reactant ratio, and space velocity were fixed at 50 bar, 16, and 2.0 h⁻¹, respectively, and the reaction temperature was changed from 233 to 247 °C by controlling based on the temperature of the catalyst bed inside the reactor. Regardless of the change in the reaction temperature, the conversion of the feed applied to the actual reactant, which was produced from palm oil to n-paraffin in the hydrotreating process, reached 100%, but the result is not shown in the graph. Also, in Fig. 11, it was shown the liquid products recovered after hydrocracking, total hydrocarbons, and the yield of C18-C16 paraffins corresponding to the composition of bio-aviation fuel, and the iso/n-paraffin ratio with the change of reaction temperature in the upgrading process using 0.5PZ catalyst. As a result, the yield of liquid products, hydrocarbons, and C18-C16 paraffins corresponding to the composition of bio-aviation fuels was not significantly affected by the reaction

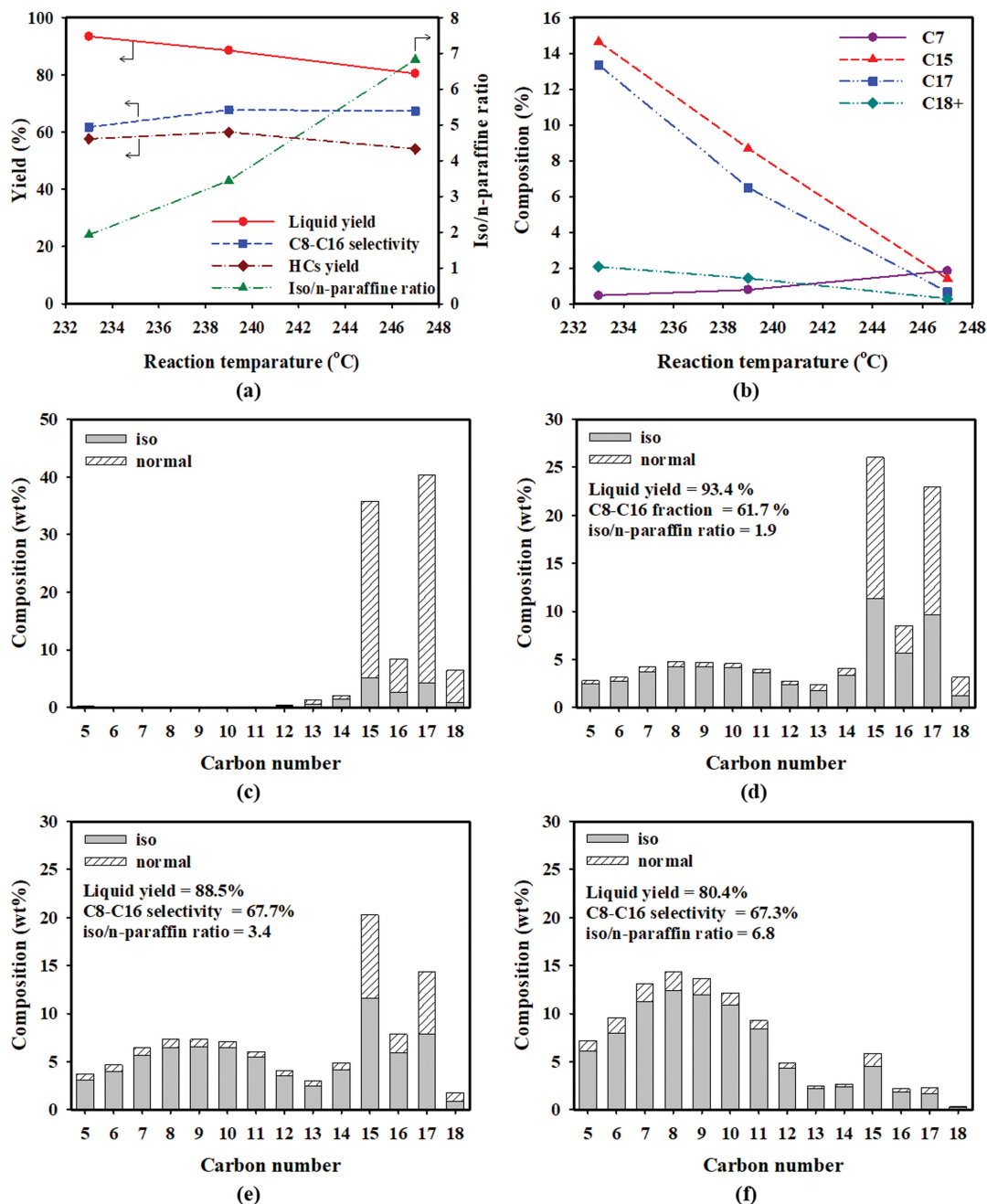
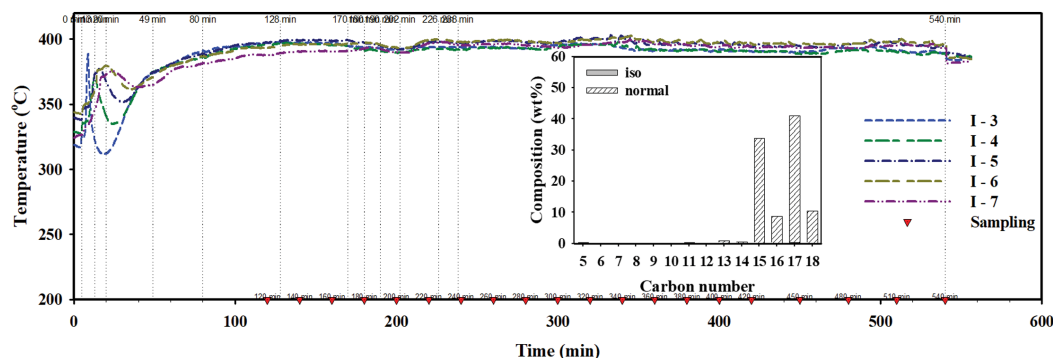


Fig. 11. Effect of reaction temperature on the reaction characteristics for a bench-scale upgrading process using 0.5PZ catalyst ((a) Yield of liquid product, hydrocarbons, bio-jet fraction, and iso/n-paraffin ratio, (b) selectivity of hydrocarbon with carbon number, (c) reactant, (d) 233 °C, (e) 239 °C, (f) 247 °C, reaction pressure: 50 bar, H_2 /reactant ratio: 16, space velocity (WHSV): 2.0 h^{-1}).

temperature change. It can be seen that the yield of liquids, hydrocarbons, and C18-C16 paraffins decreases finely as the reaction temperature increases, while the iso/n-paraffin ratio increases significantly. This result is considered to be due to the high dependence of the isomerization on the reaction temperature, although the hydrocracking and isomerization proceeded simultaneously in the controlled reaction temperature range in the upgrading process using the 0.5PA catalyst. In addition, the carbon number distribution and the iso and n-paraffin composition of the hydrocarbon obtained after the reaction significantly changed with the change

of the reaction temperature. In particular, with the increase of the reaction temperature, the C15~ paraffin selectivity of 15 or more carbon number significantly decreased, while the ~C7 paraffin selectivity of 7 or less carbon number increased. Therefore, in the upgrading process using the 0.5PA catalyst, it can be seen that the reaction temperature affects the C8-C16 paraffin yield, i.e., the bio-aviation fuel yield, and greatly affects the iso/n-paraffin ratio. Therefore, it can be seen that the reaction temperature affects the yield of C8-C16 paraffin corresponding to bio-aviation fuel and greatly affects the iso/n-paraffin ratio related to bio-aviation fuel proper-



Elapsed time (min)	120	140	160	180	200	220
iso/n-paraffin ratio	0.01	0.01	0.01	0.01	0.01	0.01
Liquid yield (%)	84.3	82.5	88.5	81.0	81.5	84.8
HCs yield (%)	81.2	79.2	85.5	77.5	78.3	78.3
~C15 selectivity (%)	2.6	3.9	2.9	8.9	2.5	2.4
C15~C18 selectivity (%)	93	93.2	92.3	93.6	93.6	93.5
C18~ selectivity (%)	4.3	2.9	4.8	3.5	3.9	4.1

Fig. 12. Catalyst bed temperature and product composition with elapsed time for long-term operation stability of the bench-scale hydrotreating process using IPA catalyst (Reaction temperature: 385 °C, reaction pressure: 40 bar, H₂/reactant ratio: 32, space velocity (WHSV): 2.0 h⁻¹).

ties in the upgrading process using the 0.5PA catalyst. In this section, the yield of C8-C16 paraffin and the iso/n-paraffin ratio corresponding to the bio-aviation fuel components of 67.3% and 6.8, respectively, were secured at 247 °C for the upgrading process using the 0.5PZ catalyst.

Fig. 12 shows the catalyst bed temperature and product composition with elapsed time for long-term operation stability of the bench-scale hydrotreating process using IPA catalyst. In Fig. 12, the long-term operation stability was investigated with controlling the reaction temperature and exothermic reaction heat by hydrogenation, catalyst performance, and obtaining paraffinic products to be used as actual reactants in the upgrading process in the bench-scale hydrotreating process using IPA catalyst. The reaction temperature, reaction pressure, H₂/reactant ratio, and space velocity were 385-395 °C, 40 bar, 32 and 2.0 h⁻¹, respectively, and the amount of catalyst charged was about 90 g. Fig. 12 includes the temperature of the catalyst bed inside the reactor monitored along with controlling reaction temperature and exothermic reaction heat in the hydrotreating process operation with IPA catalyst. As shown in Fig. 12, the monitored reaction temperature range was largely divided into three types. The first temperature zone is an exothermic reaction heat control zone, where palm oil and H₂ supplied as raw materials are simultaneously supplied to the catalyst layer, thereby controlling the temperature at which the temperature of the catalyst bed inside the reactor rises rapidly due to the heat of exothermic reaction along with hydrogenation. The second temperature zone is for setting the reaction temperature after controlling the heat of exothermic reaction. In this zone, the temperature of the catalyst bed inside the reactor reaches the desired reaction temperature after controlling the heat of exothermic reaction. The third temperature region is a reaction temperature stabilization region, and while the exothermic reaction heat is controlled, the temperature of the catalyst bed inside the reactor is stably maintained for a long time within a desired reaction tempera-

ture region, and a paraffin product is stably obtained. In the temperature range of the first exothermic reaction heat control, the temperature of the catalyst bed inside the reactor rapidly increased due to the heat of exothermic reaction along with hydrogenation for about 20 min immediately after the raw materials palm oil and H₂ were supplied. After that, the temperature of the catalyst bed inside the reactor was controlled by controlling the heat of exothermic reaction for about 30 minutes. In the temperature range of reaching the second reaction temperature, after controlling the heat of exothermic reaction, the temperature of the controlled catalyst bed in the reactor reached the desired reaction temperature of 385 to 395 °C for about 70 minutes. In the third reaction temperature stabilization section, after about 120 minutes, the temperature of the catalyst bed inside the reactor was stably maintained within the desired reaction temperature range of 385-395 °C. In addition, Fig. 12 for the hydrotreating process using IPA catalyst includes that the temperature of the catalyst bed inside the reactor was stabilized and maintained in the desired reaction temperature range of 385-395 °C through exothermic reaction heat control. Thereafter, in the stabilization reaction temperature section, it was confirmed that the supplied palm oil was continuously converted to a paraffinic product with the same composition and yield that could be used as an actual reactant in the upgrading process.

Fig. 13 shows the catalyst bed temperature and product composition with elapsed time for long-term operation stability of the bench-scale upgrading process using 0.5PZ catalyst. In Fig. 13, the long-term operation stability was investigated with controlling the reaction temperature and exothermic reaction heat by hydrogenation, control catalyst performance and the conversion of paraffinic reactants applied as reactants after being produced from actual palm oil by the hydrotreating process in the bench-scale upgrading process using 0.5PZ catalyst. The reaction temperature, reaction pressure, H₂/reactant ratio, and space velocity were 243-247 °C, 50 bar, 16.8, and 2.0 h⁻¹, respectively, and the amount of catalyst

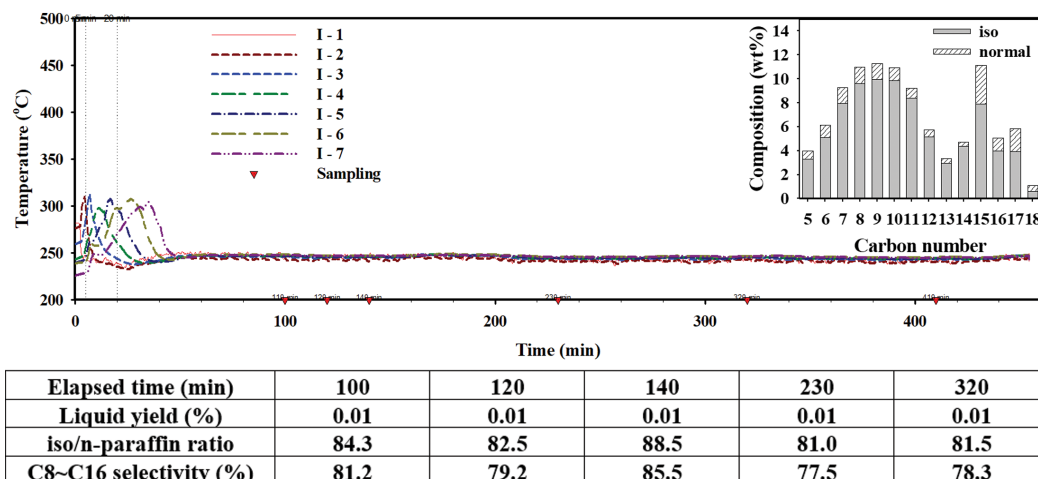


Fig. 13. Catalyst bed temperature and product composition with elapsed time for long-term operation stability of the bench-scale upgrading process using 0.5PZ catalyst (Reaction temperature: 243–247 °C, reaction pressure: 50 bar, H₂/reactant ratio: 16.8, space velocity (WHSV): 2.0 h⁻¹).

charged was about 60 g. Fig. 13 includes the temperature of the catalyst bed inside the reactor monitored along with the reaction temperature and exothermic reaction heat control in the upgrading process operation using 0.5PZ catalyst. As shown in Fig. 13, the monitored reaction temperature range was largely divided into three types. The first temperature zone is an exothermic reaction heat control zone, in which n-paraffin-based reactants and H₂ supplied as raw materials are simultaneously supplied to the catalyst bed, and the temperature of the catalyst bed inside the reactor rapidly rising by the heat of exothermic reaction along with hydrogenation is controlled. The second temperature zone is for setting the reaction temperature after controlling the heat of exothermic reaction. After controlling the heat of exothermic reaction, the temperature of the catalyst bed inside the reactor reaches the desired reaction temperature. The third temperature region is a reaction temperature stabilization region, and while the exothermic reaction heat is controlled, the temperature of the catalyst bed inside the reactor is stably maintained for a long time within a desired reaction temperature region, and a paraffin product is stably obtained. In the temperature range of the first exothermic reaction heat control, the temperature of the catalyst bed inside the reactor rapidly increased due to the heat of exothermic reaction along with hydrogenation for about 30 min immediately after the raw materials n-paraffin-based reactant and H₂ were supplied. Then, the temperature of the catalyst bed inside the reactor was controlled by controlling the heat of exothermic reaction for about 10 minutes. In the temperature range of reaching the second reaction temperature, the temperature of the catalyst bed in the reactor controlled after controlling the heat of exothermic reaction reached a desired reaction temperature of 243–247 °C for about 20 minutes. In the third reaction temperature stabilization section, after about 70 minutes, the temperature of the catalyst bed inside the reactor was stably maintained within the desired reaction temperature range of 243–247 °C. In addition, as shown in Fig. 13, in the hydrotreating process using 0.5PZ catalyst, the temperature of the catalyst bed inside the reactor was stabilized and maintained in the desired

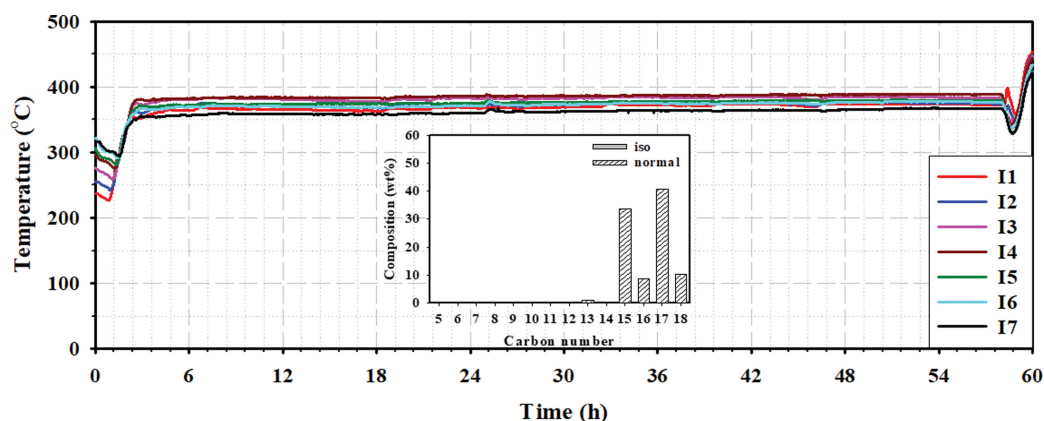
reaction temperature range of 243–247 °C through exothermic reaction heat control. Thereafter, it was confirmed the n-paraffin-based reactants supplied were continuously converted to a paraffin-based product, including a bio-aviation fuel component having the same iso/n-paraffin ratio, composition, and yield through stable and continuous hydrocracking and isomerization proceeding with hydrogenation in the stabilization reaction temperature section.

5. Facility Operation to Manufacture the Bio-aviation Fuel Prototype

Fig. 14 shows the catalyst bed temperature and product composition with elapsed time for long-term operation stability of the pilot-scale hydrotreating process using 1PA catalyst. In Fig. 14, the long-term operation stability was investigated with controlling the heat of exothermic reaction and reaction temperature and catalyst performance by hydrogenation in the pilot scale hydrotreating process using 1PA catalyst, and obtaining paraffinic products to be used as actual reactants in the upgrading process. The reaction temperature, reaction pressure, H₂/reactant ratio, and space velocity were 385–395 °C, 40 bar, 32 and 2.0 h⁻¹, respectively, and the amount of catalyst charged was about 900 g. The operating time of the hydrotreating process for preparing a paraffinic product to be used as an actual reactant in the upgrading process was about 60 h. Fig. 14 includes the temperature of the catalyst bed inside the reactor monitored along with the heat of exothermic reaction and reaction temperature control in the hydrotreating process operation with 1PA catalyst. As shown in Fig. 14, the monitored reaction temperature region is largely divided into three sections: an exothermic reaction control region, a reaction temperature setting region, and a reaction temperature stabilization region. In the temperature range of the first exothermic reaction heat control, the temperature of the catalyst bed inside the reactor rapidly increased due to the heat of exothermic reaction along with hydrogenation for about 0.5 h immediately after the feedstock palm oil and H₂ were supplied. Then, the temperature of the catalyst bed inside the reactor was controlled by controlling the heat of exothermic reaction for about 1 h. In the temperature range of reaching the sec-

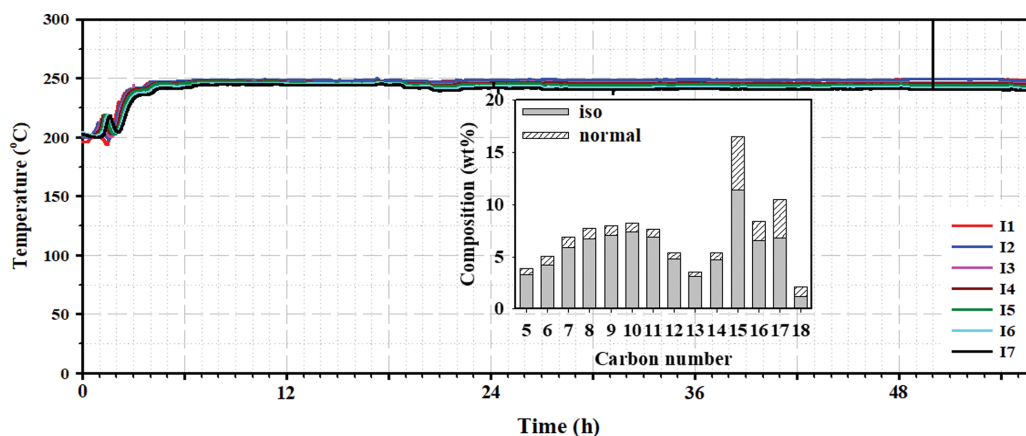
ond reaction temperature, the temperature of the catalyst bed in the reactor controlled after the exothermic reaction heat was controlled reached a desired reaction temperature of 385 to 395 °C for about 1 h. In the third reaction temperature stabilization section, after about 2.5 h, the temperature of the catalyst bed inside the reactor was stably maintained for 52 h within the desired reaction

temperature range of 385-395 °C. In addition, as shown in Fig. 14, the temperature of the catalyst bed inside the reactor was stabilized and maintained in the desired reaction temperature range of 385-395 °C through exothermic reaction heat control in the hydrotreating process using 1PA catalyst. Thereafter, in the stabilization reaction temperature section, it was confirmed that the sup-



Elapsed time (h)	4	12	24	38	48	57
iso/n-paraffin ratio	0.010	0.010	0.012	0.013	0.013	0.015
Liquid yield (%)	85.3	84.3	83.5	81.3	82.6	83.9
HCs yield (%)	80.9	81.3	82.6	79.9	80.3	81.6
~C15 selectivity (%)	2.3	2.4	2.5	2.6	2.7	2.9
C15~C18 selectivity (%)	93.7	93.3	93.7	93.5	93.1	92.4
C18~ selectivity (%)	4.0	4.3	3.9	3.9	4.2	4.6

Fig. 14. Catalyst bed temperature and product composition with elapsed time for long-term operation stability of the pilot-scale hydrotreating process using 1PA catalyst (Reaction temperature: 385 °C, reaction pressure: 40 bar, H₂/reactant ratio: 32, space velocity (WHSV): 2.0 h⁻¹).



Elapsed time (h)	6	30	48
iso/normal ratio	11.14	7.08	9.02
Liquid Recovery (%)	77.7	80.7	78.03
C8~ fraction (%)	15.31	14.16	13.72
C8~C16 fraction (%)	75.56	73.50	74.57
C16+ fraction (%)	9.13	12.34	11.71

Fig. 15. Catalyst bed temperature and product composition with elapsed time for long-term operation stability of the pilot-scale upgrading process using 0.5PZ catalyst (Reaction temperature: 243-247 °C, reaction pressure: 50 bar, H₂/reactant ratio: 16.8, space velocity (WHSV): 2.0 h⁻¹).

plied palm oil was continuously converted to a paraffinic product with the same composition and yield that could be used as an actual reactant in the upgrading process. Although there was some difference depending on the elapsed time, the yield of the liquid product reached about 77 to 80%, and the selectivity of C15-C18 paraffin, which can be used as a reactant for hydrolysis and isomerization in the upgrading process, reached about 92-94%. The C18+ paraffin selectivity of 18 or more carbon number was about 4%, and the C4-C15 paraffin selectivity of the relatively low carbon number was about 2.3%.

Fig. 15 shows the catalyst bed temperature and product composition with elapsed time for long-term operation stability of the pilot-scale upgrading process using 0.5PZ catalyst. In Fig. 15, the long-term operation stability was investigated with the control of exothermic reaction heat and reaction temperature by hydrogenation and catalyst performance, and for the conversion of paraffinic feed applied as a reactant converted from palm oil by the hydro-treating process in a pilot-scale hydrotreating process using 0.5PZ catalyst. The reaction temperature, reaction pressure, H₂/reactant ratio, and space velocity were 243-247 °C, 50 bar, 16.8 and 2.0 h⁻¹, respectively, and the amount of catalyst charged was about 600 g. The operation time of the upgrading process for producing a paraffinic product including a bio-aviation fuel component from the paraffinic raw material prepared by the hydrotreating process was

about 56 h. Fig. 15 includes the temperature of the catalyst bed inside the reactor monitored along with the heat of exothermic reaction and reaction temperature control in the upgrading process operation using 0.5PZ catalyst. As shown in Fig. 15, the monitored reaction temperature region is largely divided into three sections: an exothermic reaction control region, a reaction temperature setting region, and a reaction temperature stabilization region. In the temperature range of the first exothermic reaction heat control, the temperature of the catalyst bed inside the reactor rapidly increased due to the heat of exothermic reaction along with hydrogenation for about 0.5 h from immediately after the raw material n-paraffin and H₂ were supplied. Then, the temperature of the catalyst bed inside the reactor was controlled by controlling the heat of exothermic reaction for about 1 h. In the temperature range of reaching the second reaction temperature, after controlling the heat of exothermic reaction, the temperature of the catalyst bed in the controlled reactor reached the desired reaction temperature of 243 to 249 °C for about 1 h. In the third reaction temperature stabilization section, after about 2.5 h, the temperature of the catalyst bed inside the reactor was stably maintained for 52 h within the desired reaction temperature range of 243-249 °C. In the reaction temperature stabilization section, it was confirmed that the supplied C15-C18 paraffin material was converted to paraffin, including the bio-aviation fuel component of C8-C16 in the

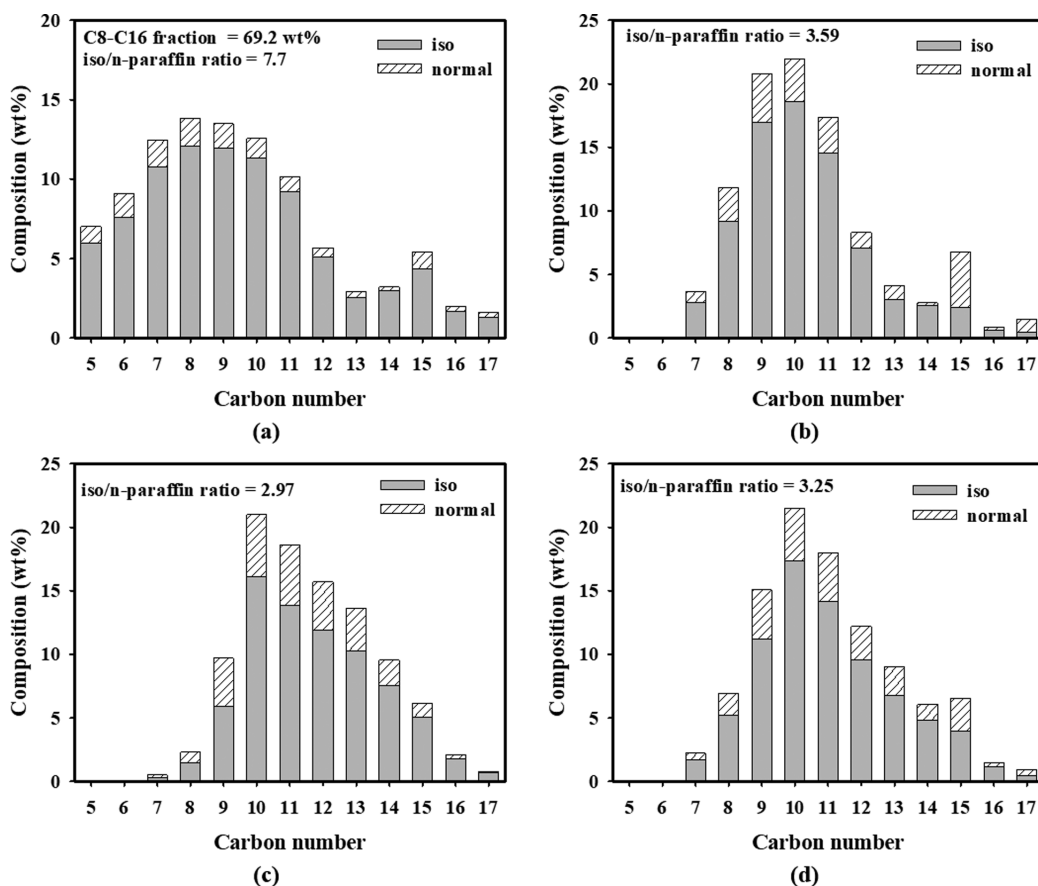


Fig. 16. Carbon number distribution of upgrading product, bio-aviation fuel, commercial Jet A-1, and 50 vol% blended bio-aviation fuel ((a) Upgrading product, (b) commercial Jet A-1, (c) 100% bio-aviation fuel, (d) 50 vol% blended bio-aviation fuel mixed with Jet A-1).

upgrading process, and thus it was continuously converted to a paraffin-based product with the same composition and yield. Although there was some difference depending on the elapsed time, the yield of the liquid product reached about 77 to 81%, and the selectivity of the paraffin product of C8-C16, a bio-aviation fuel component, reached about 73-75%. C16+ paraffin selectivity with 16 or more carbon number was about 9-12%, and ~C8 paraffin selectivity with 8 or less carbon number was about 13-15%. The iso/n-paraffin ratio, which is related to the properties of bio-aviation fuel, ranged from about 7 to 11.

6. Separation and Fuel Properties of Bio-aviation Fuel for ASTM Specification

Fig. 16 shows the carbon number distribution corresponding to

paraffinic composition of the paraffin product produced from the upgrading process, the bio-aviation fuel corresponding to C8-C16 paraffin selectively separated through the distillation process, the commercial petroleum-based Jet A-1, and 50 vol% blended bio-aviation fuel mixed with Jet A-1. Their compositions were, qualitatively and quantitatively, analyzed by GC chromatography. The paraffinic product prepared by the upgrading process showed an even distribution of carbon numbers from C5 to C18. Most of the C5-C14 paraffin components, which are a relatively low carbon number range generated by the hydrocracking in the upgrading process, were most, and the C9 paraffin components were most highly distributed. In addition, iso-paraffins converted from n-paraffins by isomerization were mainly included, so the iso/n-paraf-

Table 4. Fuel properties of 100% bio-aviation fuel and 50% blended bio-aviation fuel mixed with Jet A-1

Property	Test method	100% Bio-aviation fuel		50% Blended bio-aviation fuel		
		Requirements	Result	Requirements	Result	
Acidity, total (mg _{KOH} /g)	ASTM D3242	Max. 0.015	0.005	Max. 0.10	0.004	
Aromatics (%v/v)	ASTM D6379	-	-	Max. 25	9.4	
Sulfur, total (%m/m)	ASTM D4294	-	-	Max. 0.30	0.096	
Sulfur, mercaptan (%m/m)	ASTM D3227	-	-	Max. 0.003	0.0005	
Distillation	10% Recovered (°C)	Max. 205	167.7	Max. 205	166.8	
	50% Recovered (°C)	Report	193.1	Report	193.5	
	90% Recovered (°C)	Report	239.3	Report	239.9	
	Final boiling point (°C)	Max. 300	254.3	Max. 300	260.1	
	Residue (%)	Max. 1.5	1.2	Max. 1.5	1.2	
	Loss (%)	Max. 1.5	0.6	Max. 1.5	0.4	
Part 1	Flash point (°C)	ASTM D56	Min. 38	42.0	Min. 38	42.0
	Density (kg/m ³ , @15 °C)	ASTM D4052	730 to 772	751	775 to 840	776
	Freezing point (°C)	ASTM D7153	Max. -40	-43.6	Max. -47	-48.6
	Viscosity (mm ² /s @-20 °C)	ASTM D445	-	-	Max. 8.0	3.7
	Net heat of combustion (MJ/kg)	ASTM D4809	-	-	Min. 42.8	43.3
	Smoke point (mm)	ASTM D1322	-	-	Min. 25.0	31.0
	Copper strip (2 h @100 °C)	ASTM D130	-	-	Max. No.1	1
	THERMAL STABILITY (2.5 h @260 °C)	Filter pressure drop (mmHg)	ASTM D3241	Max. 25	0.0	Max. 25
Annex A1 VTR (VTR color code)			Less than 3	<1	Less than 3	<1
Existent gum (mg/100 ml)	ASTM D381	Max. 7	<1	Max. 7	<1	
Electrical conductivity (pS/m)	ASTM D2624			50 to 600	52	
Microseparator (Rating)	Without electrical conductivity additive	ASTM D3948	-	-	Min. 85	-
	With electrical conductivity additive		-	-	Min. 70	70
Distillation	T50-T10 (°C)	ASTM D86	-	-	Min. 15	27
	T90-T10 (°C)		-	-	Min. 40	73
Part 2	Aromatics (%v/v)	ASTM D6379	-	-	Min. 8	9.4
	Lubricity (mm)	ASTM D5001	-	-	Max. 0.85	-
	Viscosity (mm ² /s @-40 °C)	ASTM D445	-	-	Max. 12	8.03

ASTM D7566 for Detailed Batch Requirements; SPK from Hydroprocessed Esters and Fatty Acids

ASTM D7566 for Detailed Requirements of Aviation Turbine Fuels Containing Synthesized Hydrocarbons

fin ratio was about 11.33. There was a difference in quantitative values for each iso and n-paraffin component corresponding to the detailed carbon number distribution of the bio-aviation fuel component. However, it was known that the carbon number distribution range was within 7-17, and the (i+n)-paraffin, which has a carbon number distribution of about 8-15, occupied a fairly high distribution. In addition, the highest content of (i+n)-paraffin had a carbon number of 10, and the iso/n-paraffin ratio was about 3.59. Petroleum-based Jet A-1 aviation fuel had a composition similar to that of 100% bio-aviation fuel, but the iso/n-paraffin ratio of Jet A-1 was about 2.97, which contained slightly less iso-paraffin than 100% bio-aviation fuel. The general carbon number distribution corresponding to the 50 vol% mixed bio-aviation fuel component is in the range of C8 to C16, but the carbon number distribution is in the range of C7 to C17 in the actual analysis results. The main carbon number range of the blended bio-aviation fuel ranged from 8 to 15, and the highest carbon number of (i+n)-paraffin was 10. In addition, its iso/n-paraffin ratio was about 3.25. From these results, the carbon number distribution and composition of the petroleum-based Jet A-1 aviation fuel, the bio-aviation fuel produced from the HEFA process and 50 vol% blended bio-aviation fuel mixed with Jet A-1 were almost similar. Also, it can be seen that their physical properties are also expected not to be significantly different.

As described in the experimental section above, bio-aviation fuel for turbine engine testing was prepared from synthetic mixed bio-crude oil, which was produced from palm oil through hydrotreating-upgrading process, using a distillation process operating under the operating conditions shown in the table. Table 4 shows the measurement results of detailed fuel property items that can confirm the conformity of the fuel properties corresponding to the ASTM specification standard for 100% bio-aviation fuel produced by the distillation process and 50 vol% blended bio-aviation fuel manufactured by mixing petroleum-based Jet A-1 fuel and bio-aviation fuel prototype manufactured in this study. As a result, it can be seen that the fuel properties of the 100% bio-aviation fuel prototype manufactured in this study satisfy the quality standards of all items included in ASTM D7566. In addition, from these results, the operating conditions of the distillation process described in the experimental section are suitable for manufacturing a bio-aviation fuel prototype for turbine engine testing from the mixed bio-crude produced in the hydrotreating-upgrading process. Also, as a result, the fuel properties of the 50 vol% blended bio-aviation fuel also satisfy the quality standards for the properties of the ASTM D7566 standard.

CONCLUSIONS

In this study, the following was performed to obtain a technology for manufacturing bio-aviation fuel from palm oil through the HEFA process in which the catalytic hydrotreating and upgrading processes are applied as elemental processes. To secure the HEFA process technology for self-manufacturing bio-aviation fuel prototypes for turbine engine testing, it is intended to secure the catalysts required for the bio-aviation fuel manufacturing process and the operating conditions of the HEFA process equipment using these

catalysts. In the laboratory-scale hydrotreating-upgrading process, appropriate catalysts were used to investigate reaction characteristics, and long-term performance stability was tested to ensure the applicability of these catalysts. In the bench-scale hydrotreating-upgrading process to which these catalysts were used, the operating conditions were secured by investigating the reaction characteristics, and the long-term operation stability of the hydrotreating-upgrading process equipment was secured under the secured operating conditions. In the pilot-scale hydrotreating-upgrading process that applied the operating conditions and long-term operation acquired at the bench scale, the operation stability of long-term facility was secured to stably manufacture bio-aviation fuel prototypes. In this series of processes, the hydrotreating process using the 1PA catalyst and the upgrading process using the 0.5PZ catalyst were sequentially operated at the laboratory, bench, and pilot scale, respectively, to obtain a technology capable of stably manufacturing mixed bio-crude oil including bio-aviation fuel. The reaction temperature, reaction pressure, space velocity, and H_2 /reactant ratio secured as optimal operating conditions in the hydrotreating process using 1PA catalyst were 385-395 °C, 40 bar, 2.0 h⁻¹, and 32, respectively. In addition, the reaction temperature, reaction pressure, space velocity and H_2 /reactant ratio applied as optimal operating conditions in the upgrading process using 0.5PZ catalyst were 243 to 247 °C, 50 bar, 2.0 h⁻¹ and 16.8, respectively. From this, it was possible to manufacture a bio-aviation fuel prototype from a mixed bio-crude containing bio-aviation fuel components through a distillation process operated under appropriate operating conditions. The manufactured bio-aviation fuel and 50 vol% blended bio-aviation fuel were obtained with fuel properties suitable for the quality standards of ASTM D7566 and ASTM D1566, respectively. Therefore, it was found that the produced bio-aviation fuel and mixed bio-aviation fuel satisfy the quality standards and thus are suitable as fuel for turbine engine testing. In conclusion, we have secured the catalysts required for the HEFA process for bio-aviation fuel manufacturing and the process facility operation technology using these catalysts by ourselves, and manufactured bio-aviation fuel suitable for turbine engine testing while having physical properties that meet ASTM quality standards.

REFERENCES

1. ICAO (International Civil Aviation Organization), *CORSIA States for Chapter 3 State Pairs* (2020).
2. S. Kang, *Korean Chem. Eng. Res.*, **57**, 620 (2019).
3. S. R. Shabanian, S. Edrisi and F. V. Khoram, *Korean J. Chem. Eng.*, **34**, 2188 (2017).
4. H. Lee, Y.-M. Kim, I.-G. Lee, J.-K. Jeon, S.-C. Jung, J. D. Chung, W. G. Choi and Y.-K. Park, *Korean J. Chem. Eng.*, **33**, 3299 (2016).
5. H. W. Lee, H. Jeong, Y.-M. Ju and S. M. Lee, *Korean J. Chem. Eng.*, **37**, 1174 (2020).
6. Y. Lee, H. Shafaghat, J.-K. Kim, J.-K. Jeon, S.-C. Jung, I.-G. Lee and Y.-K. Park, *Korean J. Chem. Eng.*, **34**, 2180 (2017).
7. IRENA (International Renewable Energy Agency), *Biofuels for Aviation: Technology Brief* (2017).
8. Tony Radich, EIA (U.S Energy Information Administration), *The Flight Paths for Biojet Fuel* (2015).

9. W.-C. Wang, L. Tao, J. Markham, Y. Zhang, E. Tan, L. Batan, E. Warner and M. Bidy, NREL (National Renewable Energy Laboratory), *Review of Biojet Fuel Conversion Technologies* (2016).
10. DOE (U.S Department of Energy), *Alternative Aviation Fuels: Overview of challenges, Opportunities, and Next Steps* (2017).
11. Borislav Kostova, DOE (U.S Department of Energy), *Current Status of Biorefining in USA* (2017).
12. J. Bosch, S. D. Jong, R. Hoefnagels and R. Slade, Aviation biofuels: strategically important, technically achievable, tough to deliver, *Imperial College London Grantham Institute Briefing Paper No 23* (2017).
13. <https://www.darpa.mil/program/biofuels>.
14. P. T. Do, M. Chiappero, L. L. Lobban and D. E. Resasco, *Catal. Lett.*, **130**, 9 (2009).
15. T. Morgan, D. Grubb, E. Santillan-Jimenez and M. Crocker, *Top. Catal.*, **53**, 820 (2010).
16. H. J. Robota, J. C. Alger and L. Shafer, *Energy Fuels*, **27**, 985 (2013).
17. B. Peng, Y. Yao, C. Zhao and J. A. Lercher, *Angew. Chem.*, **51**, 2072 (2012).
18. D. Kubicka and L. Kaluza, *Appl. Catal., A*, **372**, 199 (2010).
19. O. I. Senol, T. R. Viljava and A. O. I. Krause, *Catal. Today*, **106**, 186 (2005).
20. H. Jeong, M. Shin, B. Jeong, J. H. Jang, G. B. Han and Y.-W. Suh, *J. Ind. Eng. Chem.*, **83**, 189 (2020).
21. J. Zhang and C. Zhao, *Chem. Commun.*, **51**, 17249 (2015).
22. D. Chiamonti, M. Buffi, A. M. Rizzo, G. Lotti and M. Prussi, *Biomass Bioenergy*, **95**, 424 (2016).
23. M. Lu, X. Liu, Y. Li, Y. Nie, X. Lu, D. Deng, Q. Xie and J. Ji, *J. Renew. Sust. Energy*, **8**, 053103 (2016).
24. W. Jicong, B. Peiyan, Z. Yajing, X. He, J. Peiwen, W. Xiaoping, L. Junxu, W. Tiejun and L. Quanxin, *Energy*, **86**, 488 (2015).
25. I. H. Choi, J. S. Lee, C. U. Kim, T. W. Kim, K. Y. Lee and K. R. Hwang, *Fuel*, **215**, 675 (2018).
26. M. Saidi and A. Jahangiri, *Chem. Eng. Res. Des.*, **121**, 393 (2017).
27. K. Zhang, X. Zhang and T. Tan, *RSC Adv.*, **6**, 99842 (2016).
28. D. Verma, R. Kumar, B. S. Rana and A. K. Sinha, *Energy Environ. Sci.*, **4**, 1667 (2011).
29. S. Liu, Q. Zhu, Q. Guan, L. He and W. Li, *Bioresour. Technol.*, **183**, 93 (2015).
30. T. Li, J. Cheng, R. Huang, J. Zhou and K. Cen, *Bioresour. Technol.*, **197**, 289 (2015).
31. M. Y. Kim, J.-K. Kim, M.-E. Lee, S. Lee and M. Choi, *ACS Catal.*, **7**, 6256 (2017).
32. R. V. Chaudhari, R. Jaganathan, D. S. Kolhe, G. Emig and H. Hofmann, *Ind. Eng. Chem.*, **25**, 375 (1986).